ENTRAINMENT IN UNBROKEN STRATOCUMULUS

Hermann Gerber[1], Glendon Frick[2], and Szymon Malinowski[2]
[1] Gerber Scientific, Reston, VA 20190, USA
[2] Naval Research Laboratory, Washington, D.C. 20375, USA
[3] University of Warsaw, Warsaw 02-093, Poland

1. INTRODUCTION

In July and August of 2008 the POST (Physics of Stratocumulus Top) field study was held off the California Coast to again investigate the entrainment process in unbroken stratocumulus (Sc). This study was motivated by the earlier DYCOMS-II stratocumulus entrainment study also of unbroken stratocumulus off the California Coast (Stevens et al., 2003a). DYCOMS-II was a useful learning experience on how to measure entrainment into Sc, since it was found that the horizontal width of entrained parcels was smaller than the mounting separation of the probes on the C-130 aircraft used during DYCOMS-II, and that the probes were mounted too far from the 5-hole gust probe on the aircraft nose. These factors likely affected entrainment flux (F_e) and velocity (w_e) estimates, with the latter varying as much as a factor of four as measured with 4 co-located independent probes on the C-130 (Gerber et al, 2005; Falloona et al. 2005), making comparisons with model predictions difficult (Stevens et al., 2003b).

The aircraft chosen for POST was the fully-instrumented Twin Otter (TO) from Naval Post Graduate School (CIRPAS, Center for Interdisciplinary Remotely Piloted Aircraft Studies). Figure 1 gives a head-on photo and sketch of the TO where only the closely co-located probes related to the present study are shown. The UFT (Ultra-Fast Temperature; Haman et al., 2001; Haman et al., 2007) probe, the PVM (liquid water content (LWC), and effective radius; Gerber et al., 1994), and three probes for measuring the vapor mixing ratio (q_v) are mounted on a hard-point ring close to the nose of the aircraft that also has on it 5 holes for the gust probe. The UFT and PVM data was collected at 1000 hz. However, given the ~0.5 m separation the two probes the data was averaged to 50 hz yielding horizontal incloud resolution in the cloud of ~1 m at the TO speed of ~50 m/s. This resolution is consistent with the smallest entrainment scales observed during DYCOMS-II, and provides for the first time the opportunity to look at the microphysics and thermodynamics of individual entrained parcels.

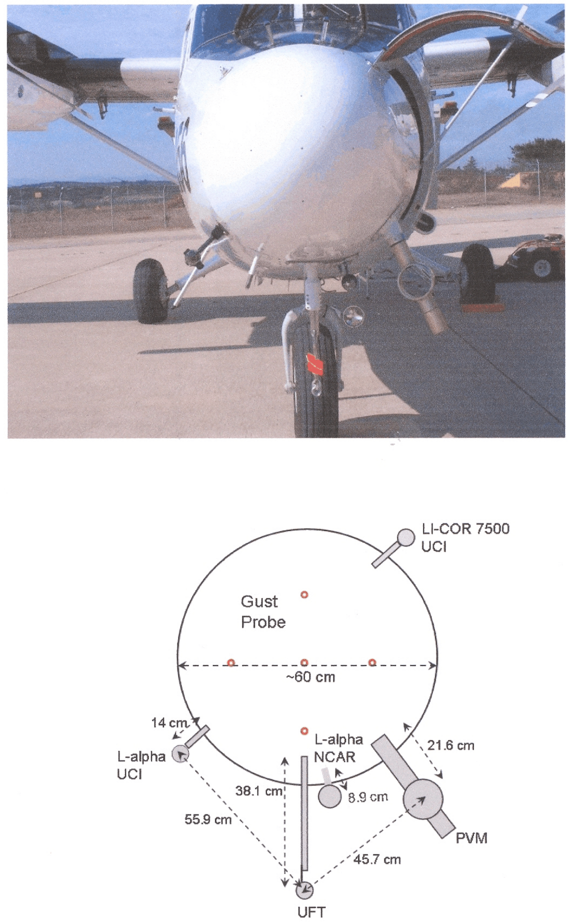

Fig. 1 - Head-on view of the CIRPAS Twin Otter (TO) research aircraft showing the locations of the UFT and PVM probes, and the q_v probes which surround the 5-hole UCI gust probe on the aircraft's nose.

The following briefly describes the measurements of w_e made during POST, the limitations found in making such measurements, the role of wind shear and mixing at cloud top, the contribution of evaporating LWC to the cooling observed in the entrained parcels, and the predictions of CTEI (cloud-top entrainment instability) and mixture fraction analysis. For greater detail see Gerber et al. (2012).

2. TWIN OTTER FLIGHT PATHS

Seventeen flights of the TO were flown out of the airport in Marina, CA located just North of Monterey. The ferry portion of most flight took the TO ~150 km WNW of Monterey Bay at which point a horizontal quasi-Lagrangian zig-zag pattern was flown so that the mean downwind location of the TO matched the mean wind speed in the Sc. A NEXSAT satellite image shown in Fig. 2

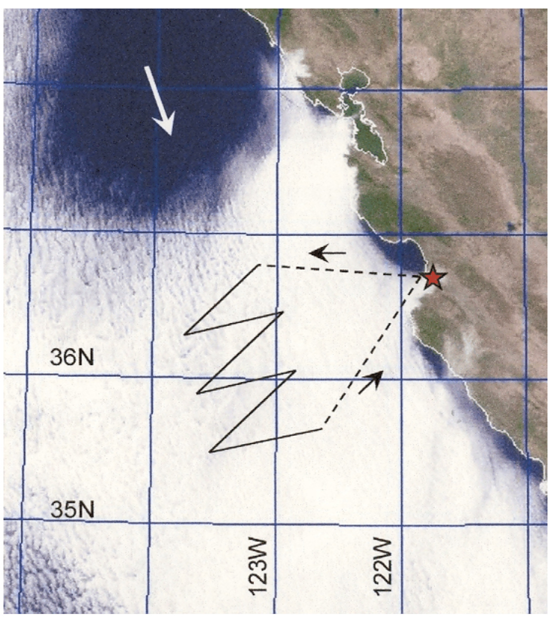

Figure 2 - Early evening NexSat satellite image of the CA coast and Pacific Ocean showing a sketch of the Twin Otter aircraft horizontal flight track for flight TO3. The white arrow shows the prevailing wind in the Sc.

illustrates a typical horizontal flight path. This path is for TO flight TO3 where a rapidly advancing area of Sc dissipation likely caused by strong shear and mixing at Sc top is seen.

The typical vertical flight path of the TO is illustrated in Fig. 3 for flight TO10. The vertical path for each TO flight concentrated on performing "saw-tooth" like profiles ranging from ~100-m above to 100-m below Sc top in order to investigate the processes associated with entrainment. In between each set ("pod") of porpoise-like profiles (Hill et al., 2012) the TO descended to near the sea surface for flux

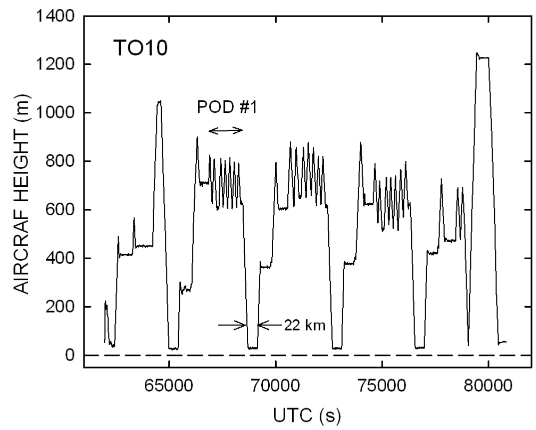

Figure 3 - Vertical flight path of the Twin Otter during flight TO10. Pods represent series of porpoises from 100-m above cloud top to 100-m below cloud top.

measurements. Horizontal legs were also flown just below cloud base and in the cloud for the same purpose. At least one higher profile was also included.

3. ENTRAINMENT MEASUREMENTS

The classical "flux-jump" equation (Lilly, 1968) often used for estimating the average entrainment velocity is given by

$$w_e = \langle w \times \phi \rangle / \Delta\phi \qquad (1)$$

where *w* is the vertical velocity, ϕ is the scalar conserved during entrainment, and $\Delta\phi$ is the jump of the scalar across the inversion separating Sc top from the free atmosphere. The numerator of Eq. (1) is termed the entrainment flux (F_e); and the brackets indicate an average.

POST provided an opportunity to evaluate the application of Eq. (1). Three factors are considered: 1) The jump of the scalar is strong (as indicated by the title of Lilly's paper). 2) The entrainment flux is linear with respect to height below Sc top to permit extrapolation of *Fe* to Sc top where w_e is calculated. 3) Entrained parcels descend in the Sc.

The scalar used in this study is the total water mixing ratio q_t. Factor No. 1) is not met for all POST flights causing large uncertainties for the value of w_e. On occasion moist layers are found adjacent to Sc top making the denominator of Eq. (1) quite small. Further, it is difficult to find the upper limit of the jump for several flights. Factor No. 2 is not met by several POST flights where F_e changes rapidly near Sc top; see the example in Fig. 4. This

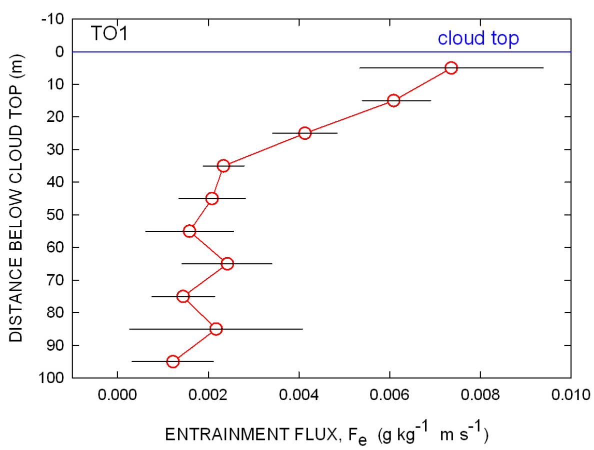

Figure 4 - Entrainment flux, F_e as a function of distance below cloud top for flight TO1 showing the non-linearity of the flux with height.

behavior occurs for several daylight flights (about half of the total POST flights are daylight flights) as well as for one night-time flight.This result has implication on previous attempts to determine w_e from measurements made lower in the Sc. The observations dealing with factor No. 3 are surprising in that entrained parcels not only descend in the Sc but also ascend. This is likely caused by mixing at Sc top where entrained parcels are fragmented by the turbulence. Figure 5 shows an example of this effect for flights TO3 and TO10 where a positive LWC contribution to *Fe* indicates entrained parcels with depleted LWC that are descending.

The method applied here to estimate w_e

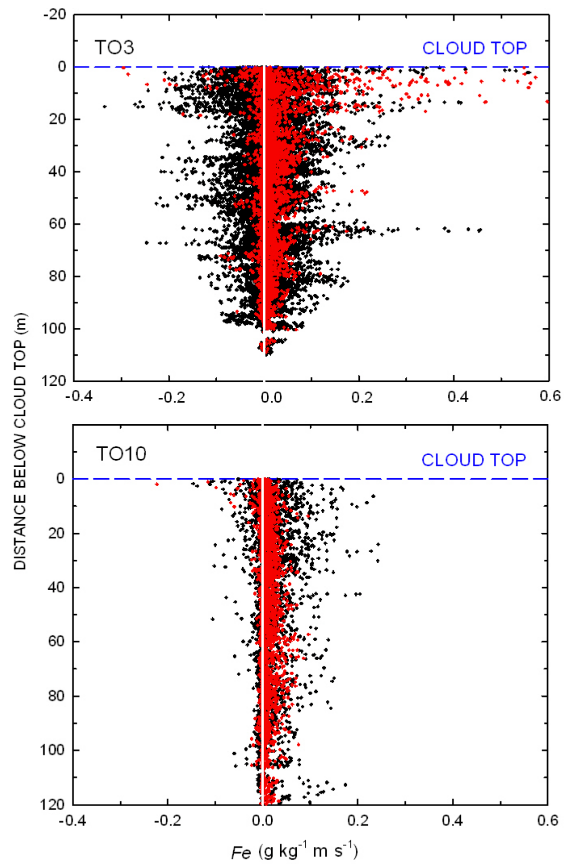

Figure 5 - Entrainment flux F_e as a function of distance below cloud top for flights TO3 and TO10; red is the flux from q_v and black is the flux contribution from LWC. The pattern for TO3 indicates strong mixing of the entrained parcels.

uses a variation of the flux-jump method where conditional sampling is used to identify the entrained parcels. The “indicator variable” (Khalsa, 1993) used for this identification are the high rate LWC measurements. Figure 6 shows an example of picking out the entrained parcels which uses the assumption that the sharp deviations of LWC from a approximately steady LWC background are the entrained parcels. Given that the q_t scalar needs both LWC and q_v in the entrained parcels, q_v is calculated by applying the Clausius-Clapeyron equation and assuming that q_v is equivalent to the saturation mixing ratio. This approach is necessary since the q_v probes on the aircraft nose were unable to provide fast data.

Figure 7 shows the calculated values of w_e for the POST flights as a function of the wind shear measured just above cloud top. The

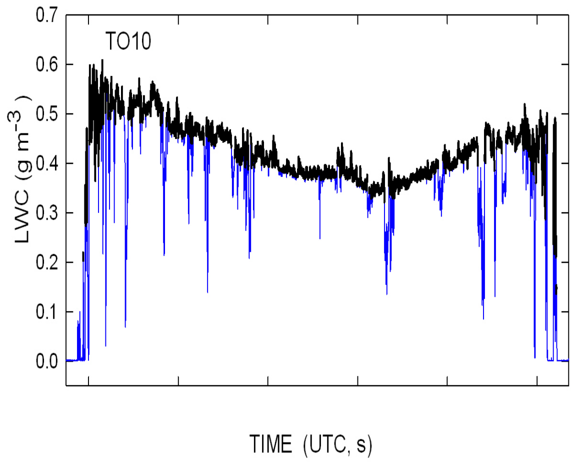

Figure 6 - High rate LWC measurements for one porpoise into the Sc from flight TO10 showing the background LWC values (black) and the location of the entrained parcels identified by conditional sampling (blue).

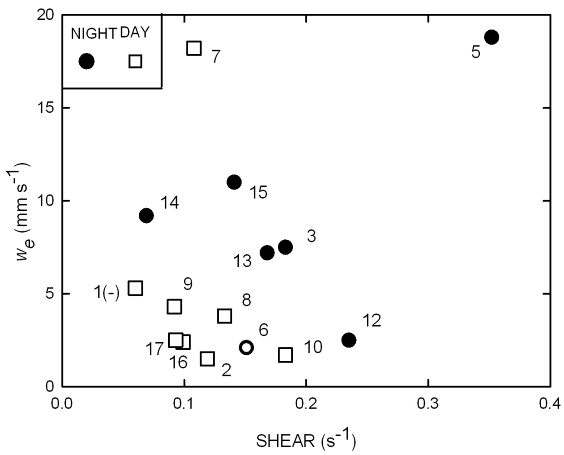

Figure 7 - Average entrainment velocity for all Sc POST flights (numbered) as a function of wind shear measured above cloud top. A higher overcast existed for night flight TO6.

correlation between the two parameters is poor suggesting that wind shear does not enhance entrainment by a significant degree. For a different result see Wang et al. (2008). Correlations made between w_e and other parameters measured on the aircraft (not shown) also give poor correlations).

4. MICROPHYSICS

An expanded segment of Flight TO is shown in Fig. 8 where temperature deviations from a slowly varying temperature background are compared to locations (red) identified as entrained parcels. The correlation between the temperature deviations and the entrained parcels is strong,

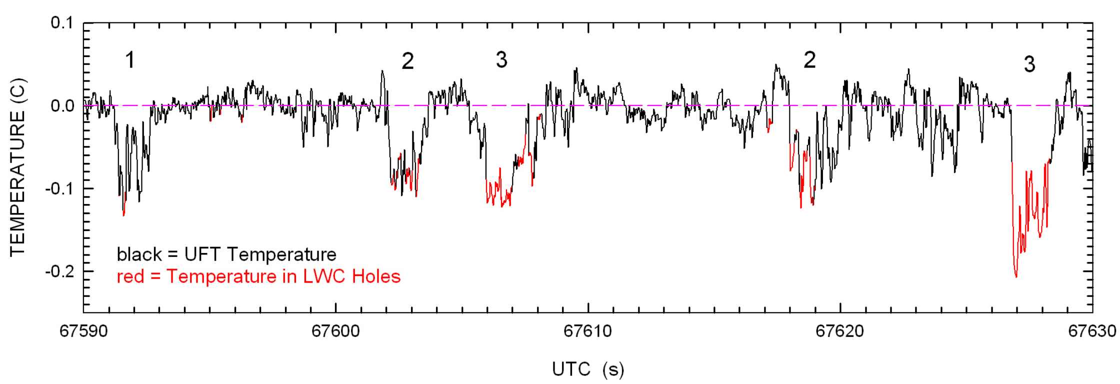

Figure 8 - Expanded segment of flight TO10 showing negative temperature deviations from the background temperature (black) and the location of the entrained parcels identified by conditional sampling of the LWC data (red); 1-m resolution data. See text for explanation of the numbers.

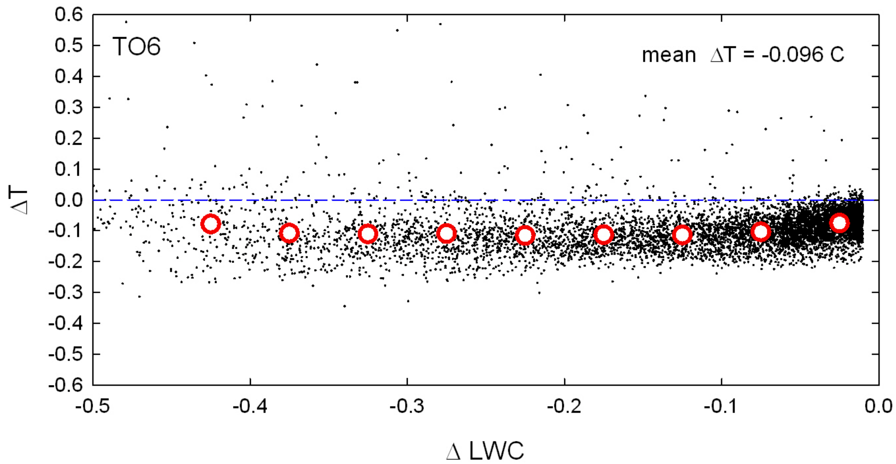

Figure 9 - Change of temperature in the entrained parcels as a function of depleted LWC in the entrained parcels for flight TO6. The red circles indicate average values.

which is also the case in the other POST flights except in some flights near Sc top. The numbers in Fig. 8 indicate how much of the segments with temperature deviation are filled with entrained parcels. Note that the number 1 indicates empty segments, 2 indicates partially filled segments with entrained parcels, and 3 indicates fully filled. Also the segments with temperature deviation are usually broader than the entrained parcels. The lack or partial presence of entrained parcels in the reduced temperature segments suggests that cooling due to droplet evaporation in the entrained parcels is minimal, and that the cooling must be due to radiative cooling. This behavior is observed both for daytime and nighttime flights.

Another way to illustrate the cooling effects is shown in Fig. 9 for flight TO6 where the temperature change in the reduced temperature segments is related to the decrease of LWC found in the segments. Mixture fraction analysis predicts the largest buoyancy reversal for POST flight TO6 with a decrease in temperature of several tenths of one degree. If cooling due to LWC evaporation plays a significant role it should show up in Fig. 9 as an increase in the loss of LWC for an increase in the cooling. The cooling in Fig. 9 is nearly constant again suggesting a minimal role for evaporative cooling and a major role for radiative cooling.

Using equations given in Stevens (2002) for mixture fraction analysis of "saturated buoyancy perturbations" the predicted temperature change resulting from mixing cloudy air near Sc top with free atmospheric air above the inversion is calculated for all POST flights and shown in Fig. 10 compared to the average observed temperature change in the entrained parcels.

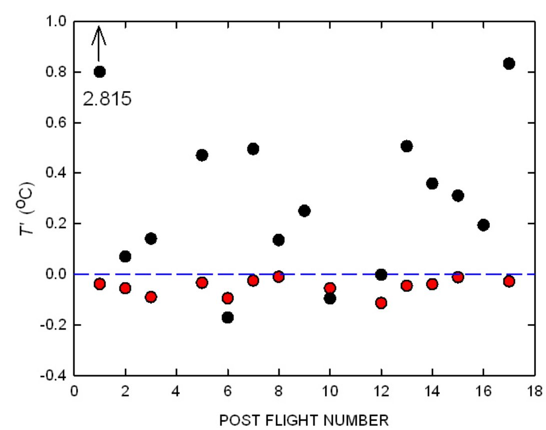

Figure 10 - The observed average change (red) in temperature T' in the entrained parcels and the predicted temperature change (black) in the parcels using mixture fraction analysis.

The correlation in Fig. 10 is poor, with the predicted temperatures changes generally indicating warming due to the mixing, and with the observed temperatures changes showing slight cooling or near isothermal mixing. Calculation of CTEI for all the flights also suggests that most flights should show warming in saturated mixtures.

A key assumption in mixture fraction analysis and CTEI calculations is that cloudy air near Sc top mixes with air from the free atmosphere above the inversion. The observations in POST suggest that this assumption does not hold, and that cloudy air mixes with pre-conditioned inversion air caused by detrainment of sensible heat and evaporation of cloud water as proposed earlier (Gerber et al., 2002, 2005). While the predictive equations must be correct, they need to use much smaller jumps consistent with the pre-conditioning to explain the lack of cooling in the entrained parcels due to LWC evaporation; see Malinowski et al. (2012) for further discussion of this topic.

5. CONCLUSIONS

1) The application of the “flux-jump” approach to estimate the entrainment velocity (w_e) requires a linear entrainment flux below cloud top which is not always observed in the POST Sc.

2) The jump of the conserved scalar (q_t) across the inversion, needed to estimate w_e, is often difficult to determine in the Sc, as has been also noted in previous studies. This leads to significant uncertainty in w_e.

3) The aircraft measurement of entrainment flux [(numerator of Eq. (1)] gives more robust numbers than the jump measurements and should be used for model inter-comparisons.

4) All POST flights show wind shear above cloud top, with some showing strong shear and mixing causing significant droplet evaporation.

5) Cooling in segments of cloud which have a high correlation with entrained parcels is caused primarily by radiative cooling and at most by a minimal amount by LWC evaporation.

6) Entrained parcels appear to be nearly buoyancy neutral and fill various portions of radiatively cooled parcels and with an unknown mechanism.

7) Effective radius in entrained parcels is nearly constant compared to unaffected cloud suggesting that mixing is either inhomogeneous or homogenous if the entrained air is pre-conditioned to be moist and near isothermal. The latter appears to be the case for POST Sc.

8) Predictions of CTEI and buoyancy changes (mixture fraction analysis) are incorrect for POST Sc because of wind shear and mixing at Sc top, and because the predictions make use of entire jumps across the inversion rather than jumps that are a fraction of the entire jumps.

9) The observations show that moisture flux goes both ways across the cloud-top interface. Theory is missing to include this phenomena likely caused by wind shear, mixing, and droplet evaporation.

10) Another field study of unbroken Sc is recommended with a longer observation period than for POST. More flights with better meso-scale coverage is desired.

11) POST data is available that are suitable for high-resolution inter-comparisons between LES and measurements (see http://www.eol.ucar.edu/projects/post/).

6. ACKNOWLEDGMENTS

POST was a collaborative effort of about two dozen participants. All are thanked for their efforts. Haf Jonsson the TO chief scientist and Mike Hubbell the TO pilot have special thanks for making the POST experience at CIRPAS outstanding and a pleasure. H. Gerber, G. Frick, and S. Malinowski were supported by NSF for the POST field study (ATM-07355121).

7. REFERENCES

Faloona, I., D. H. Lenschow, T. Campos, B. Stevens, M. C. VanZanten, B. Blomquist, D.

Thornton, A. Bandy, and H. Gerber, (2005): Observations of entrainment in Eastern Pacific marine stratocumulus using three conserved scalars. *J. Atmos. Sci., 62*, 3268-3285.

Gerber, H., B. G. Arends, and A. S. Ackerman, (1994): New microphysics sensor for aircraft use. *Atm. Res., 31*, 235-252.

Gerber, H., S. P. Malinowski, J.-L. Brenguir, and F. Burnet, (2002): On the entrainment process in stratocumulus clouds. *Proc. 11th Conf. On Cloud Physics*, Ogden, UT, Amer. Meteor. Soc., CD-ROM, paper JP7.6

Gerber, H., S. P. Malinowski, J.-L. Brenguier, and F. Burnet, (2005): Holes and entrainment in stratocumulus. *J. Atmos. Sci., 62*, 443-459.

Gerber, H., G. Frick, S. Malinowski, H. Jonsson, D. Khelif, and S. Krueger, (2012): Entrainment in unbroken stratocumlulus. *J. Geophys. Res., Atm.*, submitted.

Haman, K. E., S. P. Malinowski, B. Strus, R. Busen, and A. Stefko, (2001): Two new types of ultra-fast aircraft thermometer. *J. Atmos. Oceanic Technol., 18*, 117-134.

Haman, K. E., S. P. Malinowski, M. J. Kurowski, H. Gerber, and J.-L. Brenguier, (2007): Small scale mixing processes at the top of a marine stratocumulus - A case study. *Quart. J. Roy. Meteor. Soc., 133*, 213-226, doi10.102/qj.5.

Hill, S., S. Krueger, H. Gerber, and S. Malinowski, (2012): Entrainment and mixing in stratocumulus-topped boundary layers during POST. *Extended abstract in 16th ICCP*; paper P.2.40.

Khalsa, S. J. S., (1993): Direct sampling of entrainment events in a marine stratocumulus layer. *J. Atmos. Sci., 50*, 1734-1750.

Lilly, D. K., (1968): Models of cloud-topped mixed layers under a strong inversion. *Quart. J. Roy. Meteor. Soc., 94*, 292-309.

Malinowski, S., K. Nurowska, M. Kopec, W. Kumala, H. Gerber, and D. Khelif, (2012): Turbulent inversion and entrainment into stratocumulus toped boundary layer. *Extended abstract in 16th ICCP*, paper P.2.12.
.

Stevens, B., (2002): Entrainment in stratocumulus toped mixed layers. *Quart. J. Roy. Meteor. Soc., 128*, 2663-2690.

Stevens, B., and Coauthors, (2003a): Dynamics and chemistry of marine stratocumulus - DYCOMS II. *Bull. Amer. Meteor. Soc., 84*, 579-593.

Stevens, B., and Coauthors, (2003b): On entrainment rates in nocturnal marine stratocumulus. *Quart. J. Roy. Meteor. Soc., 129*, 3469-3493.

Wang, S., J.-C. Golaz, and Q. Wang, (2008): Effect of intense wind shear across the inversion on stratocumulus. *Geophys. Res. Lett., 35*, L15814, doi:10.1029/2008GL033865.